JOURNAL OF APPLIED POLYMER SCIENCE VOL. 19, PP. 939–949 (1975)

Behavior of Unstretched Nylon 6 Fibers Subjected to Longitudinal and Transverse Impact

E. CERNIA and W. CONTI, *Snam Progetti S.p.A., Direzione Generale Ricerca e Sviluppo, S. Donato Milanese, Milan, Italy*

Synopsis

The impact resistance of unstretched fibers of nylon 6 has been measured at impact velocities in the range of 10–20 m/sec by means of a freely falling dart of variable weight. The analysis was made on fibers with a high moisture content, since samples with low moisture content were brittle, as were unstretched fibers of poly(ethylene terephthalate). The observed impact behavior is in line with that predicted by the stress–strain curves obtained on a dynamometer, although it deviates somewhat in the ultimate properties and when the extent of deformation is small. The behavior for small deformations is discussed and a model is proposed.

INTRODUCTION

The behavior of various synthetic fibers subjected to both longitudinal and transverse impact has been extensively studied both experimentally and theoretically.[1] For the experimental studies, some very sophisticated apparatus capable of recording the details of the phenomenon even at very high impact velocities of the order of the speed of sound has been developed.[2] The theoretical studies have sought to interpret the impact behavior in terms of the stress–strain curves, and thus to predict the propagation velocities of the various wavefronts of deformation.[3] In both the experimental and the theoretical studies, only stretched fibers (generally of high modulus) have been considered, and at very high impact velocities—probably for reasons inherent in the practical applications. On the contrary, no studies have been made on unstretched fibers, whose ability to absorb large amounts of energy with large increase in length should make them of interest in applications where it is desired to dissipate irreversibly a large quantity of energy without excessive deacceleration such as would be required for guard rails or similar applications. The stress–strain curve of an unstretched fiber measured previously with load increasing and then decreasing shows a high degree of hysteresis in which only a fraction of the energy supplied is later restored.

In the impact phenomenon, the velocity of propagation of the tension in the medium plays an important role and involves the inertia of the medium itself. For impact velocities close to the speed of sound, a correct approach to the problem must take the inertia of the medium into account, thus leading to extremely difficult differential equations, since for unstretched fibers terms of a dissipative character must be considered. At velocities much lower than the

speed of sound, howeve, it is possible to neglect inertial forces and the difficulty of the problem is drastically reduced.

The phenomenological interpretation of the experimental data requires that the result of the impact experiment, expressed in terms of the energy imparted (E) and the resulting strain suffered by the fiber (γ_f), be related to the stress–strain curve of the material.

Provided the velocity is not too high, the energy is given by

$$E = \int_0^{\gamma_f} T \, d\gamma = \int_0^{t_f} T\dot{\gamma} \, dt$$

where T is the tension (from the stress–strain curve) and t_f is the time required to reach the new equilibrium. Theoretically, the energy absorbed will depend not only on those physical quantities that generally influence the tension T (extension, rate of deformation, time, etc.) but, because of the term in $\dot{\gamma}$, will also depend on the history of the deformation. It is to be expected, therefore, that the energy will differ according to whether the impact occurs transversely or longitudinally. In the event that the tension T depends only on the elongation, however, the energy will no longer depend on the history of the deformation and the two types of impact will lead to the same result.

In this work, the impact behavior of an unstretched fiber of nylon with high moisture content will be analyzed in relation to the stress–strain curves obtained on a dinamometer at low rates of deformation. Some slight differences in the behavior of the fiber during the impact tests with respect to that predicted by the stress–strain curves will be pointed out.

EXPERIMENTAL

Apparatus

High-impact velocities were achieved by means of a freely falling dart of variable weight having the form shown in Figure 1a. The dart is composed of an external shell (a) and a variable number of lead discs (g), which could be used to vary the total weight of the dart. The external shell was fitted with four arms through which holes were drilled to carry the guides (c) consisting of a pair of taut monofilaments of nylon. The additional weights (b) were held firmly together by a pressure nut (d). The weight of the dart could be varied from 50 g to 400 g.

The fiber sample was placed in the path of the falling dart as shown in (e) and (f) of Figure 1b, and fixed at the extremities to rigid supports. In arrangement (e), the impact occurred transversely, while in arrangement (f), it occurred longitudinally.

The dart was released electromagnetically from heights varying up to 20 m from the point of impact with the fiber, corresponding to a theoretical impact velocity of 20 m/sec.

The actual impact velocity was measured by a photocell detecting system placed close to the point of impact. This device consisted of two projectors each emitting a narrow, collimated beam of light and placed at a distance of 10 cm apart. In front of these projectors were placed two photocells that opened and closed, respectively, an electronic circuit by means of which it was possible to measure the time taken for the dart to intercept the two light beams with a preci-

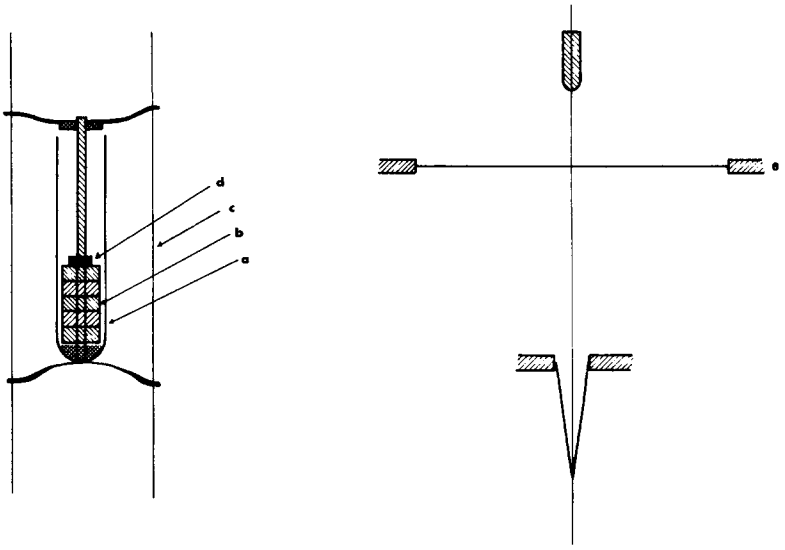

Fig. 1. left, Dart: (a) external shell; (b) weights; (c) guides; (d) pressure. right, Impact arrangements: (e) transverse; (f) longitudinal.

sion of 5% in the most unfavorable case (maximum velocity). With this device it was possible to verify that the impact velocity was reduced from the theoretical value by varying amounts according to the height of the fall and the weight of the dart. The maximum observed reduction (fall from 20 m with minimum weight) was 20%, but for weights greater than 300 g, the observed velocities were practically equal to the theoretical values, even for a fall from 20 m.

Materials

Unstretched Nylon 6 Fiber. This thread was drawn from industrial spinning equipment operating at 280°C with a drawing ratio of 20 in the spinning tower. The relative viscosity of the fiber (1% polymer concentration in 96% sulfuric acid at 20°C) was 3.2. The systematic impact tests were performed on threads with 9% moisture content, count 3650 den, 70 filaments.

Poly(ethylene Terephthalate) Fiber. This thread was also drawn from industrial spinning equipment operating at 290°C with a drawing ratio of 26 in the spinning tower. Intrinsic viscosity 0.635 (in *o*-chlorophenol at 20°C), 1700 deniers, 70 filaments.

RESULTS

Stress–Strain Curves

The nylon fiber described above was subjected to two series of measurements on an Instron dinamometer (Model TT-CM). In the first series, the sample length was 2.5 cm, with traction velocities of 1, 5, 10, 20, and 50 cm/min. The results are shown in Figure 2, from which it may be seen that for velocities greater than 5 cm/min a plateau is formed and that in these cases the curves of tension versus elongation are practically independent of the traction velocity. After the plateau, the tension increases almost linearly with elongation.

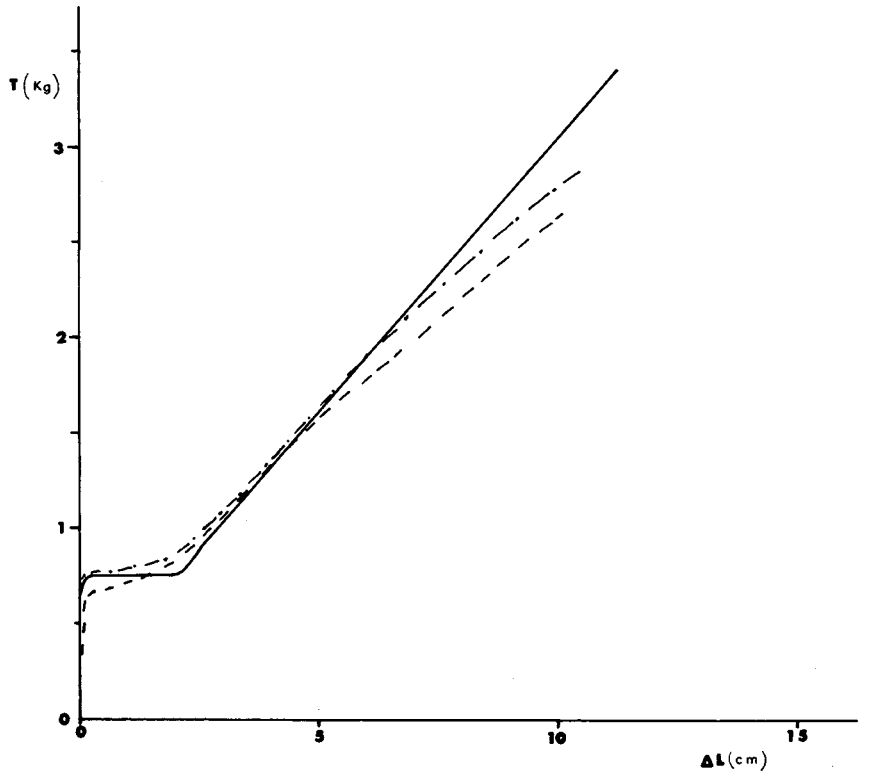

Fig. 2. Tension–elongation curves for sample of 2.5-cm length at various traction velocities: (- - - - -) 1 cm/min; (- · - · - ·) 5 cm/min; (———) 10–50 cm/min.

The second series of tests was made at the highest possible traction velocity (50 cm/min) with sample lengths of 2.5, 5, 10, and 20 cm (in the last case, the test was not continued to breaking point, the apparatus having first reached the maximum possible extension). In this case, the tensions-versus-elongation curves all differ from one another, although if the stress is plotted as a function of the relative elongation (strain) (Fig. 3, solid line), the plots do then all coincide with a single master curve.

It may be affirmed, then, that for traction velocities in the range of 10–50 cm/min (0.166–0.83 cm/sec), the tension-versus-strain curve is independent of the velocity and may be represented with sufficient accuracy by the following equations:

$$T = T_0 \qquad \text{for } \gamma = \frac{L - L_0}{L_0} < \gamma_n = \frac{L_n - L_0}{L_0}$$

$$T = T_0 + K(\gamma - \gamma_n) \qquad \text{for } \gamma > \gamma_n$$

where T is the tension for the sample extended to length L and L_0 is the initial length of the sample; L_n is the length of the sample at the end of the plateau. The constants T_0, γ_n, and K were determined to be 0.75, 0.83, and 0.71 kg, respectively.

In Figure 3 are shown (discontinuous lines) the tension–strain curves made on the same fiber with 2% moisture content, and the behavior is seen to be rather

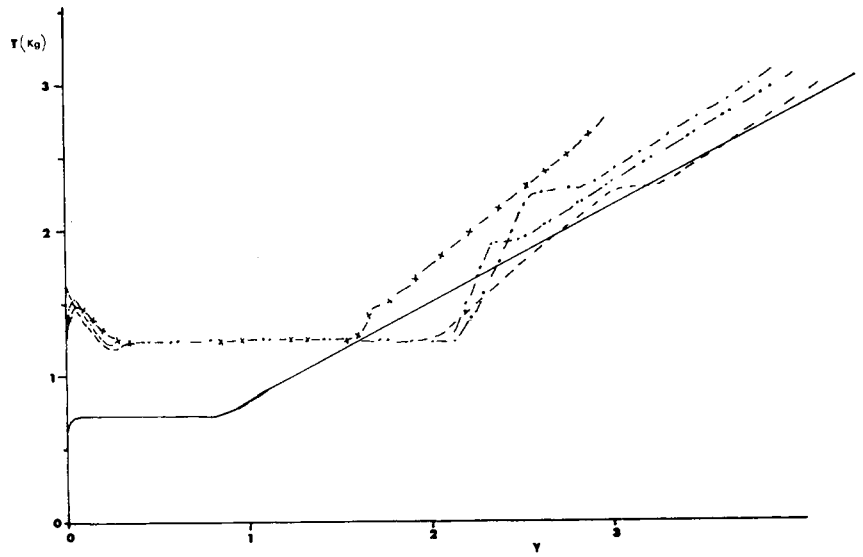

Fig. 3. Tension–strain curves: continuous line, master curve for sample with high moisture content; discontinuous lines, for sample with low moisture content at a traction velocity of 50 cm/min and various lengths: (- - -) 2.5 cm; (- · - · -) 5 cm; (- · · - · · -) 10 cm; (- x - x -) 20 cm.

different. In this case, the tension-versus-strain curves show a maximum before the plateau, while immediately after the plateau the tension increases with a steep slope that later changes abruptly to a more gentle value. For large values of L_0, and thus when the rate of deformation is low, the portion with the steep slope is longer, while the value of the slope tends to be smaller. Thus, the analysis of the tension-versus-strain curves for the fiber with low moisture content is rather more complicated in that they are dependent on the traction velocity.

It should be added for completeness that the curves for poly(ethylene terephthalate) fibers also show strong dependence on traction velocity, as is well known.[4]

Impact Tests

Exploratory tests with the apparatus described showed that fibers of poly(ethylene terephthalate) and nylon 6 with low moisture content are fragile, being able to absorb very little energy and having low elongations at the breaking point, whereas fibers of nylon 6 with high moisture content are able to absorb high-impact energies. For this reason, as mentioned in the introduction, the analysis is restricted to the nylon 6 fiber with high moisture content.

Impact tests were conducted with the dart falling from various heights (5, 10, and 20 m), with a range of dart weights (50–400 g) and sample lengths (30, 60, and 120 cm), and with longitudinal and transverse impact.

In Figure 4, the energy imparted by the dart is plotted as a function of the elongation ($\Delta L = L - L_0$) suffered by the fiber for a sample length of 60 cm in transverse impact, and for various dart weights falling from the three heights mentioned. The energy imparted was calculated by taking into account the kinetic energy of the dart ($^1/_2\ mv^2$), the final level reached by the dart, and the rebound height resulting from energy restored to the dart by the fiber. The

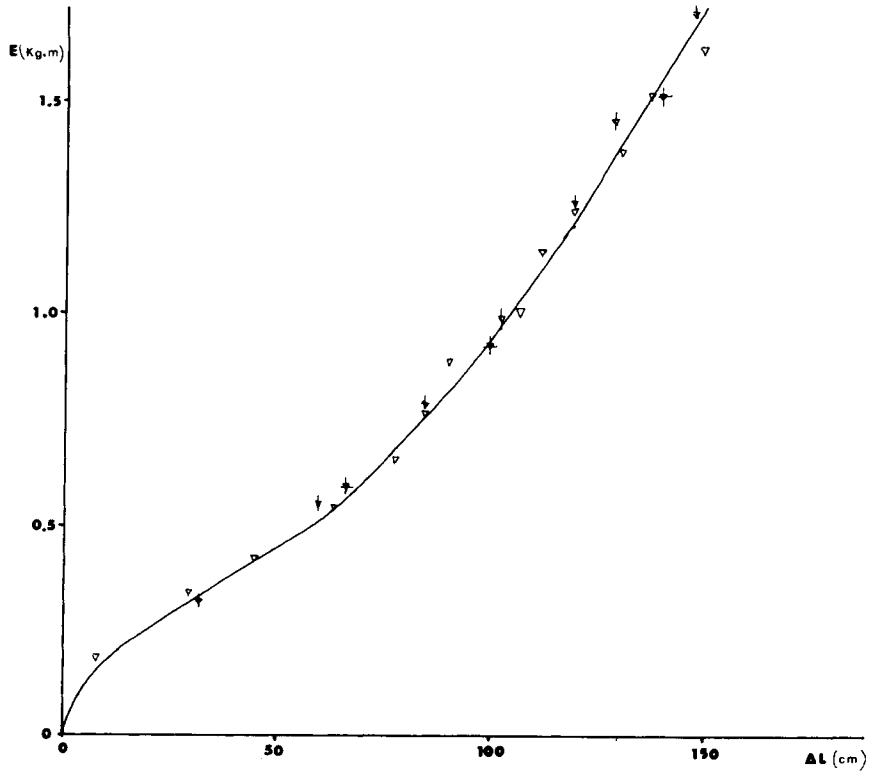

Fig. 4. Energy–elongation curves for the sample of 60 cm in transverse impact: symbols for experimental data as in Fig. 5:

rebound decreases as both the weight of the dart and the velocity of impact increase. The rebound reached values around 15% for the lowest weights and velocities (50 g and fall from 5 m).

The experimental data all fall on a single curve, demonstrating the independence of the phenomenon in this case from the velocity of impact, in analogy to what was seen for the tension-versus-elongation curves. When the sample length is varied, a single master E-versus-ΔL curve is no longer obtained, although a master curve is obtained when the energy per unit initial length E/L_0 is plotted against the relative elongation (strain) $\gamma = \Delta L/L_0$.

The experimental data for longitudinal impact fall on the same curve as those for transverse impact, provided that the energy is halved and the initial length is taken to be that of the doubled sample. Thus, a master curve is obtained by plotting the specific energy per unit volume $E_s = E/V$ as a function of the strain $\gamma = \Delta L/L_0$.

This is shown in Figure 5, in which only a part of the experimental data is given for the sake of clarity, although the solid line has been drawn taking all the data into account.

Regarding the ultimate characteristics (strain at breaking point γ_r and maximum specific energy $(E_s)_M$), it may be added that for the impact tests

$$\gamma_r = 2.6 - 2.8; \qquad (E_s)_M = 12\text{–}15 \text{ kg/cc}$$

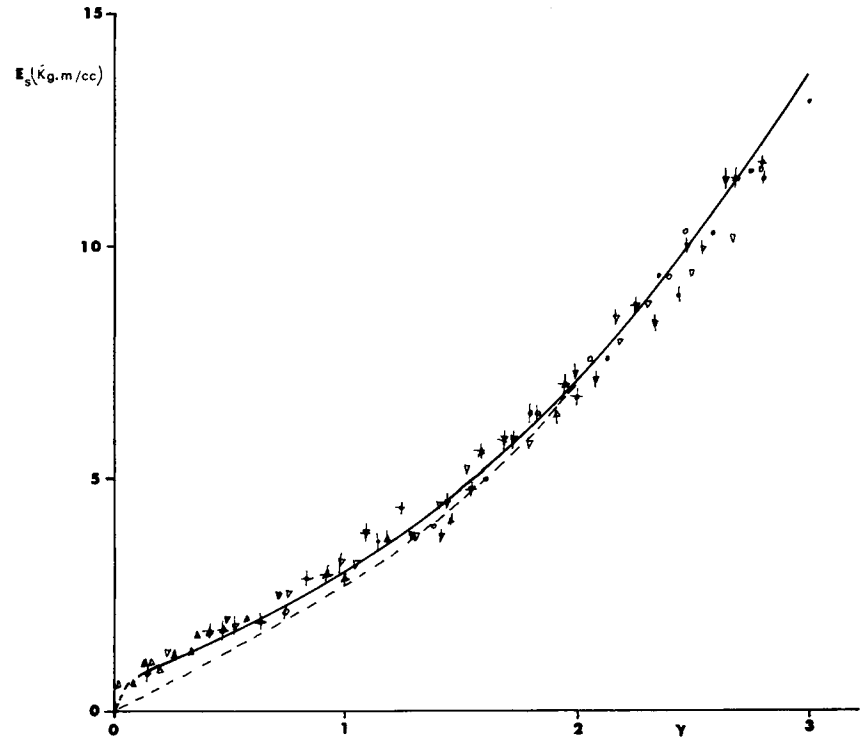

Fig. 5. Master curve of specific energy vs. strain.

Height of fall	5 m	10 m	20 m
Sample length 30 cm:			
longitudinal impact	●	●	●
transverse impact	○	○	○
Sample length 60 cm			
longitudinal impact	▼	▼	▼
transverse impact	▽	▽	▽
Sample length 120 cm			
longitudinal impact	▲	▲	▲
transverse impact	△	△	△

while for the stress–strain curves

$$\gamma_r = 4\text{–}5; \qquad (E_s)_M = 23\text{–}30 \text{ kg/cc}.$$

It is not within the scope of this paper, however, to analyze these properties.

DISCUSSION

The stress–strain curves ($\sigma = T/S_0$, $\gamma = \Delta L/L_0$) obtained on the dinamometer are practically independent of the traction velocity, just as the specific energy-versus-strain curves are independent of impact velocity, at least for $\gamma > 0.1$. It is therefore natural to compare the curve of specific energy versus γ with that calculated by integration of the stress–strain curve (broken line of Fig. 5). For large deformations ($\gamma > 2.0$), the integrated stress–strain curve coincides exactly with the specific energy curve obtained experimentally from the impact measure-

ments. For smaller deformations, the experimental curve is higher than the calculated one and has a sigmoidal form, whereas the latter is straight for $\gamma \leq \gamma_n$ and thereafter curves upward.

The sigmoid form of the specific energy-versus-strain curve suggests, obviously, that the applied force passes through a maximum at very low strains. This feature recalls the stress–strain curves of the nylon with low moisture content (Fig. 3), although no such peak is observed for the high-moisture fiber with the low rates of deformation used on the dinamometer.

The brittleness of the low-moisture nylon could therefore be interpreted in terms of the high tension, greater than the cohesive tension of the fiber that is established at small elongations in the impact tests. The fact that the high-moisture fiber shows a peak at low elongations in the impact tests but not in the dinamometer tests is all the more reason for an elevated tension peak for the low-moisture fiber, which already shows a pronounced velocity-dependent peak in the traction tests on the dinamometer.

On increasing the impact velocity, the curve of energy as a function of strain does not change substantially, and it may therefore be concluded, for the nylon fiber with high moisture content, at least, that the behavior is not explicable by the presence of any kind of viscosity-related phenomenon. It is more reasonable to think in terms of a yield point and a lowering of tension as in the case of a changeover from static to dynamic friction. Thus, in the first few moments, the impact energy is stored by the fiber in elastic form, the sample being extended uniformly along its entire length; a moment later a neck forms at one point and the accumulated energy in the filament, plus that which continues to be supplied by the dart, flows into the neck making it run right along the sample (if the available energy is sufficient), and finally the filament continues to stretch uniformly. Concerning the initial mode of energy absorption, there is some qualitative experimental evidence: the rebound of the dart is higher the smaller the extension of the fiber (i.e., the smaller the mass of the dart and the lower its velocity).

Exploratory tests with a 50-g dart falling from 5 m onto a much thicker thread (obtained by doubling the original thread several times) showed a much higher rebound (ca. 4m).

Furthermore, close examination under the microscope showed evidence for the presence of necks in fibers that had suffered only light impacts and relatively small elongation, whereas no necks were observed in fibers that had suffered large or very low elongations, thus confirming the development of the phenomenon as described above.

Since, as we have seen, a neck is formed in the thread, it is obvious that the strain must be independent of the length of the sample, although it might be expected to depend on the impact velocity. In that case, however, there must be a dependence on the natural draw ratio L_n/L_0. Within experimental error, there is no definite evidence for either of these effects. Thus, the yielding tension (σ_0) is independent of the mode of impact.

On the basis of the foregoing considerations, the behavior of the fiber can be represented by a model of the kind shown in Figure 6. The spring of modulus G represents the elastic behavior prior to the yielding. The frictional element F offers a resistance σ_M before the yielding and a resistance σ_0 once the yielding has begun ($\sigma_M > \sigma_0$). The tension falls from σ_M to σ_0 with a time constant $1/\alpha$. Finally, the second spring of modulus K represents the behavior of the fiber after

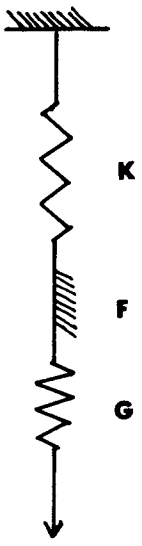

Fig. 6. Model: K and G are elastic elements; F is a frictional element.

the yielding stage; this modulus will not be a constant, but must vary with the strain in order to account for the hardening of the material. The model does not include viscous elements, since we have seen that there is no dependence on either the impact velocity (impact tests) or the traction velocity (dinamometric tests). As for the time constant $1/\alpha$, we shall see that its effect is observable only at very low strain.

Thus, for stress $\sigma < \sigma_M$, we have

$$\sigma = G \cdot \gamma.$$

For simplicity, in view of the slope of the dinamometric stress–strain curves prior to yielding, we can put $G = \infty$, i.e., there is no deformation until $\sigma > \sigma_M$.

For $\sigma > \sigma_M$, we have, with $k = A \cdot \gamma$ for simplicity

$$\sigma = (\sigma_M - \sigma_0)e^{-\alpha t} + \sigma_0 + A\gamma^2.$$

The tension $T = \sigma/(\gamma + 1)$ in the impact tests produces a deacceleration $\ddot{\gamma}$ of the dart of weight m, from which we have $T = -m\ddot{\gamma}$. Thus, we obtain the differential equation

$$m\ddot{\gamma} + \frac{\sigma_M - \sigma_0}{\gamma + 1} e^{-\alpha t} + \frac{\sigma_0 + A\gamma^2}{\gamma + 1} = 0.$$

Then, multiplying by $d\gamma$ and integrating with respect to γ, which goes from zero to the final strain γ_f corresponding to $\dot{\gamma} = 0$, we obtain

$$\frac{1}{2} mv^2 = (\sigma_0 + A) \ln (1 + \gamma_f) + A\gamma_f\left(\frac{\gamma_f}{2} - 1\right) + H \tag{1}$$

where

$$H = (\sigma_M - \sigma_0) \int_0^{\gamma_f} \frac{e^{-\alpha t}}{1 + \gamma} d\gamma.$$

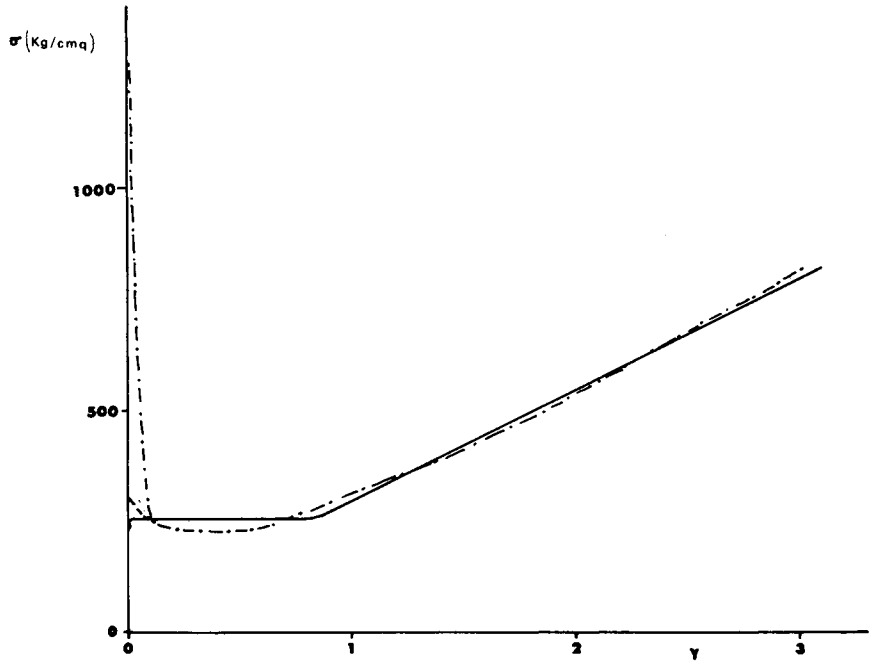

Fig. 7. Stress–strain curves from dynamometric measurements (continuous line) and from impact tests according to the complete model (dash-dotted line), and according to the model with only one type of friction (dashed line).

It is reasonable to suppose that α is large, so that the system evolves rapidly from the static to the dynamic situation. In other words, the integrand may be thought of as being already close to zero even for an infinitesimal strain $d\gamma$, and therefore

$$\int_0^{\gamma_f} \frac{e^{-\alpha t}}{1+\gamma}\, d\gamma \simeq \frac{1}{2}\delta\gamma.$$

Thus, H is a constant, independent of the impact velocity, provided that $\gamma \gg \delta\gamma$.

The continuous line in Figure 5 coincides with that given by eq. (1) with $H = 0.5$, $A = 3.33$, and $\sigma_0 = 2.69$. Considering $\delta\gamma = 0.1$, we get finally $\sigma_M = 12.7$.

Taking the derivative of eq. (1) with respect to γ_f, we obtain the tension

$$T = (\sigma_0 + A)\frac{1}{1+\gamma} + A\,(\gamma - 1). \tag{2}$$

In Figure 7, the stress–strain curves from the Instron dinamometer (solid line) are compared with the values given by eq. (2) for $\gamma > 0.1$ (dash-dotted line), while values for $0 < \gamma < 0.1$ are interpolated taking into account that $\sigma_M = 12.7$.

By allowing only one type of friction (σ_0), the value of the tension for $\gamma = 0$ would have been σ_0, that is, 269 (in the units of Fig. 7), and we would have had the behavior shown by the dashed line, which is insufficient to explain the pronounced sigmoidal effect in the E_s-versus-γ curve. Actually, even allowing only one kind of friction (σ_0), the E_s-versus-γ curve would have a slightly sigmoidal shape, but so slight as to make it indistinguishable from the E_s-versus-γ curve

obtained by integrating the dinamometric stress-strain curve (dashed line in Fig. 5).

The high value of α masks the dependence of the results on time and therefore on the velocity of the test, not only in the impact tests, but even more so in the dynamometric tests. On lowering the moisture content, α, of course, decreases, as is seen from the stress–strain curves of Figure 3, and this contributes to the brittleness of the fiber at low moisture content.

The stress–strain curve deduced from the impact tests displays a plateau of yielding lower than that obtained on the dynamometer, and this may plausibly be related to the increase in temperature suffered by the fiber as it stores, practically adiabatically, the energy supplied during the impact.

CONCLUSIONS

The unstretched fiber of nylon 6 shows a behavior toward impact in the medium velocity range that is deducible in general outline by simple integration of the stress–strain curve obtainable at low velocity on a dynamometer, and is independent of the type of impact (longitudinal or transverse). The behavior differs, however, from that calculated from the stress–strain curve in respect of the ultimate characteristics, which we have not discussed, and in the region of low deformation ($\gamma < 2$).

It is possible to interpret the observed behavior in terms of a yielding of the fiber in which the stress decays rapidly from an initial value σ_M, perhaps connected with the velocity of impact but in any case not detectable for $\gamma < 0.1$, to a dynamic value σ_0, as has been proposed elsewhere.[5]

This behavior, notably simple in that it does not involve dependence either on time or on the velocity of impact, seems to be peculiar to nylon 6 with high moisture content; at low moisture content, in fact, the fiber is brittle to impact and the stress–strain curves from the dynamometer are sensitive to the rate of deformation. The fiber of PET shows fragile behavior similar to that of nylon 6 with low moisture content.

References

1. A. G. H. Dietz and F. R. Eirich, *Appl. Polym. Symposium*, **5**, (1965).
2. W. K. Stone, H. F. Schiefer, and G. Fox, *Text. Res. J.*, **25**, 520 (1955); J. C. Smith, F. L. McCrackin, H. F. Schiefer, W. K. Stone, and K. M. Towne, *Text. Res. J.* **26**, 822 (1956).
3. J. C. Smith, F. L. McCrackin, and H. F. Schiefer, *Text. Res. J.*, **28**, 288 (1958).
4. A. B. Thompson, *J. Polym. Sci.*, **34**, 741 (1959).
5. M. Reiner, *Advanced Rheology*, H. K. Leewis, London, 1971, p. 159.

Received September 2, 1974